ARTICLE

Self-reactive CD4+ IL-3+ T cells amplify autoimmune inflammation in myocarditis by inciting monocyte chemotaxis

Atsushi Anzai[1,2]*, John E. Mindur[1]* [ID], Lennard Halle[1], Soichi Sano[3], Jennifer L. Choi[1] [ID], Shun He[1], Cameron S. McAlpine[1], Christopher T. Chan[1], Florian Kahles[1], Colin Valet[1], Ashley M. Fenn[1], Manfred Nairz[1], Sara Rattik[1], Yoshiko Iwamoto[1], DeLisa Fairweather[4] [ID], Kenneth Walsh[3], Peter Libby[5] [ID], Matthias Nahrendorf[1,6] [ID], and Filip K. Swirski[1,6] [ID]

Acquisition of self-reactive effector CD4+ T cells is a major component of the autoimmune response that can occur during myocarditis, an inflammatory form of cardiomyopathy. Although the processes by which self-reactive T cells gain effector function have received considerable attention, how these T cells contribute to effector organ inflammation and damage is less clear. Here, we identified an IL-3–dependent amplification loop that exacerbates autoimmune inflammation. In experimental myocarditis, we show that effector organ–accumulating autoreactive IL-3+ CD4+ T cells stimulate IL-3R+ tissue macrophages to produce monocyte-attracting chemokines. The newly recruited monocytes differentiate into antigen-presenting cells that stimulate local IL-3+ CD4+ T cell proliferation, thereby amplifying organ inflammation. Consequently, Il3−/− mice resist developing robust autoimmune inflammation and myocardial dysfunction, whereas therapeutic IL-3 targeting ameliorates disease. This study defines a mechanism that orchestrates inflammation in myocarditis, describes a previously unknown function for IL-3, and identifies IL-3 as a potential therapeutic target in patients with myocarditis.

Introduction

Myocarditis is an inflammatory heart disease and a primary cause of sudden death and dilated cardiomyopathy in children and young adults (Cooper, 2009; Sagar et al., 2012b; Trachtenberg and Hare, 2017; Swirski and Nahrendorf, 2018). The disease is often triggered by cardiotropic infections and is subsequently enhanced by an autoimmune response, in which inappropriately activated T cells specific to cardiac antigens damage the myocardium and propagate heart failure. A recent clinical study showing that patients with fulminant myocarditis have a more adverse outcome compared to those without the drastic inflammatory phenotype also suggests that augmented cellular immunity confers irreversible tissue injury, which causes fatal arrhythmia and cardiac dysfunction (Ammirati et al., 2017). Thus, investigating the immunopathogenic mechanisms involved in the development of autoimmune cardiac inflammation might identify new therapeutic interventions for patients with myocarditis.

An enduring concept in immunology emphasizes two discrete phases linked to the development of T cell–mediated autoimmune inflammation (Marrack et al., 2001; Rosenblum et al., 2015). During the sensitization phase, which typically occurs in the LNs, naive T cells specific for a self-antigen encounter APCs and, consequently, mature and expand. During the later effector phase, these activated T lymphocytes, along with other lymphoid and myeloid cell subsets, accumulate in their cognate antigen-expressing tissues. When the inciting antigen is a cardiomyocyte-derived peptide from a protein like the α myosin heavy chain (αMHC), inflammatory cells invade the heart, leading to myocarditis. While the first phase generates a lymphocyte pool with pathogenic potential, it is during this second phase that inflammation and irreversible organ damage actually occur.

The cellular and molecular sequelae that promote the generation of autoreactive T cells have been studied extensively in various autoimmune disease models (Goodnow et al., 2005; Kronenberg and Rudensky, 2005; Mohan and Unanue, 2012; Bluestone et al., 2015; Theofilopoulos et al., 2017). Less is known, however, about the cytokine networks that control mobilization, recruitment, and function of inflammatory cells during the effector phase. The multifunctional cytokine IL-3 promotes hema-

[1]Center for Systems Biology, Massachusetts General Hospital and Harvard Medical School, Boston, MA; [2]Department of Cardiology, Keio University School of Medicine, Tokyo, Japan; [3]Hematovascular Biology Center, Robert M. Berne Cardiovascular Research Center, University of Virginia School of Medicine, Charlottesville, VA; [4]Department of Cardiovascular Medicine, Mayo Clinic, Jacksonville, FL; [5]Cardiovascular Division, Department of Medicine, Brigham and Women's Hospital, Boston, MA ; [6]Department of Radiology, Massachusetts General Hospital and Harvard Medical School, Boston, MA.

*A. Anzai and J.E. Mindur contributed equally to this paper;   Correspondence to Filip K. Swirski: fswirski@mgh.harvard.edu.

topoiesis, leukocyte differentiation, and survival (Williams et al., 1990; Weber et al., 2015). Although the discovery of IL-3 dates back several decades (Hapel et al., 1981; Ihle et al., 1981; Yang et al., 1986), relatively little is known about the scope of IL-3's action in the context of autoimmunity, with a handful of studies on its role in type I diabetes (Ito et al., 1997), lupus nephritis (Renner et al., 2015), collagen-induced arthritis (CIA; Brühl et al., 2009; Srivastava et al., 2011), and experimental autoimmune encephalomyelitis (EAE; Hofstetter et al., 2005; Renner et al., 2016), but no studies have linked IL-3 with myocarditis. Moreover, studies that have connected IL-3 to autoimmune diseases have yielded potentially conflicting results and were not able to determine the cytokine's mechanism of action. This study shows that IL-3 is dispensable to T cell sensitization but essential to the effector phase, during which it orchestrates a tricellular amplification loop consisting of self-reactive T cells, macrophages, and monocyte-derived dendritic cells (moDCs).

Results

IL-3 exacerbates cardiac inflammation in experimental autoimmune myocarditis (EAM)

To test whether IL-3 plays a role in autoimmune inflammation observed in myocarditis, we adopted a mouse model of EAM in which myocardial inflammation is induced by immunizing genetically susceptible mice with αMHC peptide emulsified in CFA using two s.c. injections 7 d apart (Cihakova and Rose, 2008; Fig. 1 A). At 21 d after the first injection, the hearts of WT female mice developed considerable inflammation comprising intense leukocyte infiltration (Fig. 1 B), a high inflammatory score (Fig. 1 C), and elevated cardiac serum troponin I (Fig. 1 D). $Il3^{-/-}$ female mice, however, were profoundly protected from EAM, developing comparably minimal cardiac inflammation. Male $Il3^{-/-}$ mice were likewise protected from cardiac inflammation, indicating that sex was not a contributing factor to IL-3–dependent inflammation (Fairweather et al., 2013; Fig. S1 A). These dramatic differences prompted us to enumerate leukocyte recruitment to the heart at 10 d (beginning of the inflammation) and 21 d (peak of the inflammation) after the first injection. We adapted a flow cytometric procedure (Anzai et al., 2017) to identify and quantify Ly-6C^{high} monocytes/macrophages, moDCs, macrophages, plasmacytoid DCs (pDCs), classical DC1 (cDC1), cDC2, neutrophils, T cells, B cells, eosinophils, and other leukocytes (Fig. S1, B and C). We also confirmed monocytes' bipotential capacity to differentiate into both F4/80$^+$ CCR2$^+$ MHCII$^+$ macrophages and CD172a (SIRPα)$^+$ XCR1$^-$ CCR2$^+$ moDCs in the inflamed heart (Epelman et al., 2014; Clemente-Casares et al., 2017; Van der Borght et al., 2017; Fig. S1, D–F). We show that compared with WT mice, $Il3^{-/-}$ mouse hearts accumulated fewer leukocytes (Fig. 1 E), with notable decreases on day 21 among Ly-6C^{high} monocytes/macrophages, moDCs, MHCII$^+$ macrophages, pDCs, neutrophils, and T cells (Fig. 1 F), including both CD4$^+$ and CD8$^+$ cells (Fig. 1 G). Realizing that myocardial inflammation can progress to inflammatory dilated cardiomyopathy, we then evaluated cardiac fibrosis and heart function. Azan staining of mouse hearts 45 d after disease induction revealed minimal development of cardiac fibrosis among $Il3^{-/-}$ mice in comparison

to WT controls (Fig. 1 H). Moreover, echocardiography indicated that $Il3^{-/-}$ mice developed less myocardial dysfunction than WT animals (Fig. 1 I). Together, these data show that IL-3 contributes decisively to acute inflammation and chronic heart failure during autoimmune myocarditis.

T cell–derived IL-3 is essential to myocarditis

Having established the importance of IL-3 in orchestrating myocarditis, we next sought to identify IL-3's source. We measured $Il3$ by quantitative PCR (qPCR) in tissue sections collected at various time points after the first injection of αMHC/CFA. $Il3$ production was negligible to low in the steady state but increased substantially (>20-fold) in the heart on day 21, with only smaller increases in the draining LNs but not in other locations such as the bone marrow (BM), spleen, thymus, and lung (Fig. 2 A). Flow cytometry of cardiac single-cell suspensions on day 21 revealed CD3$^+$ CD4$^+$ T cells to be major sources of intracellular IL-3 (Fig. 2 B). Although ∼20% of the IL-3–producing CD4$^+$ T cells were either IFN-γ$^+$ or IL-17A$^+$ and ∼4% were IFN-γ$^+$ IL-17A$^+$, most IL-3$^+$ CD4$^+$ T cells did not produce either cytokine (Fig. 2 C). In addition, none of the IL-3$^+$ CD4$^+$ T cells produced IL-4 (Fig. 2 C). Thus, while some IL-3–producing CD4$^+$ T cells appear to be representative of the proinflammatory T helper (Th) 1 and Th17 cell lineages, which commonly associate with autoimmune inflammation (Dardalhon et al., 2008), the majority of IL-3$^+$ CD4$^+$ T cells do not actively secrete IFN-γ or IL-17A. Isolating T cells from sensitized animals and culturing them with BM-derived DCs (BMDCs) along with either αMHC or myelin oligodendrocyte glycoprotein, an antigen targeted in models of multiple sclerosis, confirmed that T cells sensitized to αMHC in vivo can secrete IL-3 protein in an antigen- and disease-specific manner upon recognizing their MHCII-restricted cognate peptide (i.e., αMHC; Fig. 2 D).

To determine the importance of IL-3–producing CD4$^+$ T cells to establishing myocardial inflammation, we pursued a two-pronged strategy. First, we isolated CD4$^+$ T cells from sensitized WT and $Il3^{-/-}$ mice and adoptively transferred those cells to SCID mice lacking functional lymphocytes (Fig. 2 E). 10 d after transfer, we noted that hearts of SCID mice receiving WT CD4$^+$ T cells accumulated more leukocytes than hearts of SCID mice receiving $Il3^{-/-}$ CD4$^+$ T cells (Fig. 2 F). Second, we generated mixed-chimeric $Rag1^{-/-}Il3^{-/-}$ mice that specifically lacked IL-3 production by lymphocytes (Fig. 2 G). Compared with $Rag1^{-/-}$ WT controls, hearts of mixed chimeras with $Il3^{-/-}$ CD4$^+$ T cells developed significantly less inflammation, as characterized by fewer Ly-6C^{high} monocytes/macrophages, moDCs, and T cells, 21 d after EAM induction (Fig. 2 H). Together, these data indicate that CD4$^+$ T cells critically influence the inflammatory phenotype that occurs during autoimmune myocarditis.

T cell sensitization does not require IL-3

Having determined that CD4$^+$ T cell–derived IL-3 promotes inflammation during myocarditis, we next addressed the mechanism. We first tested IL-3's role in sensitization, as this is the defining process during which APCs elicit expansion of antigen-specific T cells in LNs. Following a BrdU pulse, we observed that T cells in the draining LNs proliferated at higher rates in vivo 10 d after myocarditis induction, but their proliferative rate did
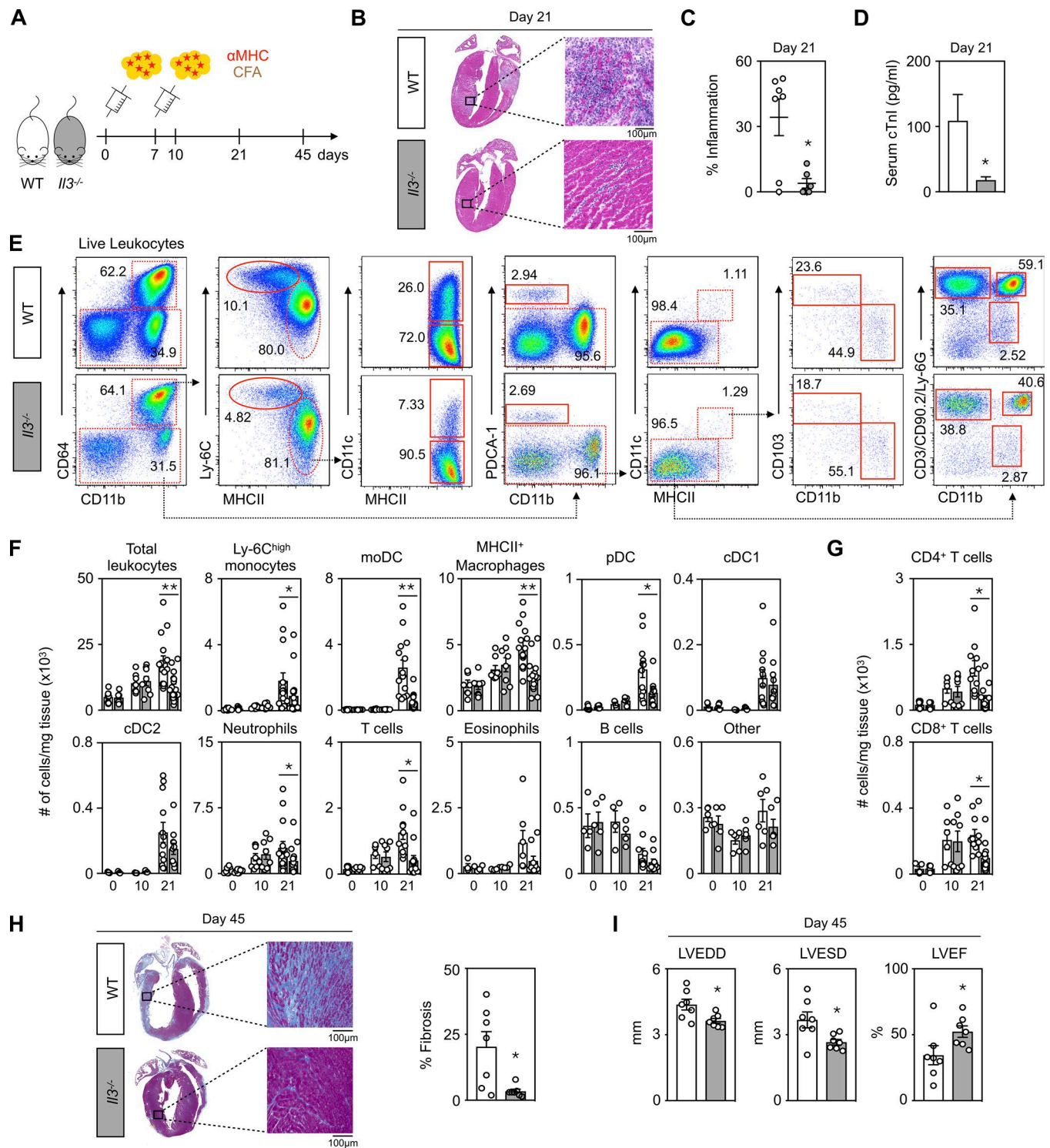
Anzai et al.
IL-3 in autoimmune myocarditis

Journal of Experimental Medicine
https://doi.org/10.1084/jem.20180722

370

Figure 1. **IL-3 exacerbates cardiac inflammation in EAM. (A)** Schematic diagram of the experimental design. EAM was induced by injecting 100 μg cardiac αMHC emulsified in CFA on days 0 and 7. Mice were killed before or 10, 21, or 45 d after the first immunization. **(B)** Representative H&E staining of the hearts from WT and *Il3*−/− mice at peak of inflammation (day 21). Bars, 100 μm. **(C)** H&E-stained sections as in B were scored for inflammation by percentage of myocardium infiltrated with mononuclear cells (*n* = 6–7 per group of two independent experiments). **(D)** Serum cardiac troponin-I (cTnI) levels in WT and *Il3*−/− mice were measured by ELISA on day 21 (*n* = 6–7 per group of two independent experiments). **(E)** Representative flow dot plots of WT and *Il3*−/− heart tissue cell suspensions to assess inflammatory cells on day 21. **(F and G)** Flow cytometry–based quantification of indicated leukocyte subsets in the hearts of WT and *Il3*−/− mice before and 10 and 21 d after the first immunization (*n* = 5–15 per group of at least two independent experiments). **(H)** Representative Azan staining of the hearts from WT and *Il3*−/− mice on day 45 and quantification of cardiac fibrosis (*n* = 7 per group of two independent experiments). Bars, 100 μm. **(I)** Assessment of cardiac diameter and function by echocardiography on day 45 (*n* = 7 per group of two independent experiments). *, P < 0.05; **, P < 0.01. For statistical analysis, a two-tailed unpaired *t* test was used, and Mann–Whitney *U* tests were applied to compare two groups. Results are shown as mean ± SEM. Error bars represent SEM.
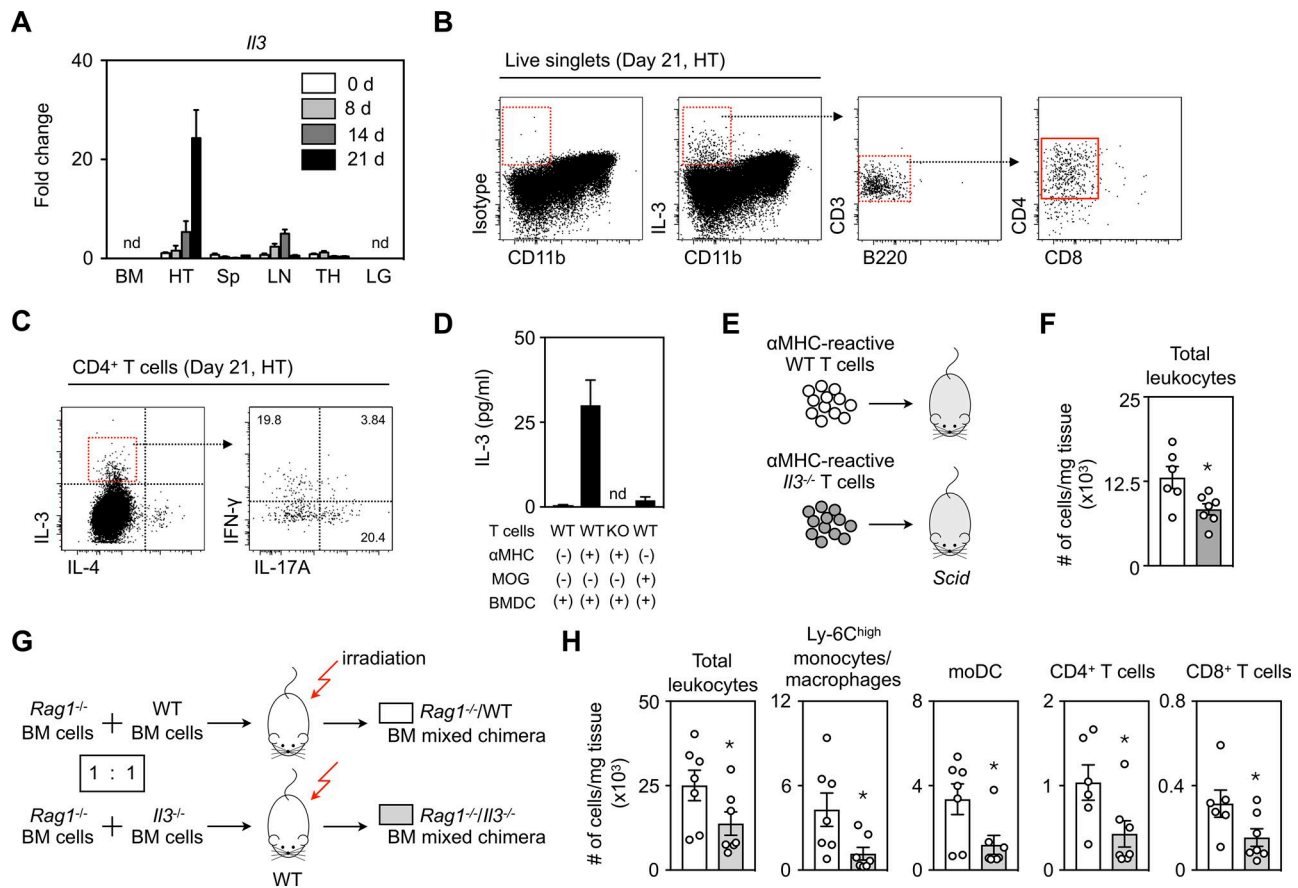
Figure 2. **T cell–derived IL-3 is essential to cardiac inflammation in myocarditis. (A)** *Il3* mRNA levels in the heart (HT), BM, spleen (Sp), draining LN, thymus (TH), and lung (LG) before and 8, 14, and 21 d after the first immunization (*n* = 6–9 per group representing two independent experiments). nd, not detected. **(B)** Representative flow dot plots of heart tissue cell suspensions to identify IL-3+ cells on day 21. **(C)** Further flow cytometric characterization of IL-3–producing CD4+ T cells by costaining for IFN-γ, IL-17A, and IL-4 in the inflamed heart. **(D)** T cells were isolated by draining LNs of either WT or *Il3*−/− immunized mice on day 14 and culturing with WT BMDCs in the presence or absence of the indicated peptide (10 µg/ml) for 72 h. Culture supernatants were collected, and IL-3 levels were measured by ELISA. MOG, myelin oligodendrocyte glycoprotein. **(E)** Schematic diagram of T cell adoptive transfer–induced EAM. **(F)** Quantification of total leukocyte numbers in the hearts of recipient *Scid* mice (*n* = 6–7 per group of two independent experiments). **(G and H)** WT mice were lethally irradiated and reconstituted with a mixture of BM cells obtained from *Rag1*−/− and either WT or *Il3*−/− mice at 1:1 ratio to generate *Rag1*−/−/WT and *Rag1*−/−/*Il3*−/− BM mixed chimeras (G). After 6–7 wk to allow for reconstitution, the mice were subjected to EAM induction, and leukocyte subsets in the heart were evaluated by flow cytometry on day 21 (H; *n* = 7–8 per group of two independent experiments). *, P < 0.05. For statistical analysis, a two-tailed Mann–Whitney *U* test or unpaired *t* test was applied to compare two groups. Results are shown as mean ± SEM.

not depend on IL-3 (Fig. 3 A). Likewise, CD4+ T cell proliferation in vitro, involving culture of T cells from sensitized animals with BMDCs, αMHC, and recombinant IL-3, indicated that proliferation required antigen, but not IL-3 (Fig. 3 B). Consequently, we failed to detect any IL-3–dependent differences in the number of CD4+ T cells in the draining LNs after myocarditis induction (Fig. 3 C). Furthermore, flow cytometric analyses showed no differences in the number of DC subsets isolated from the draining LNs, such as CD11c^high MHCII^int (resident cDCs), CD11c+ MHCII^high (migratory cDCs), and CD11b^high CD64+ CD11c+ MHCII+ (moDCs; Fig. 3, D and E). We also sought to determine whether IL-3 can alter DC APC function during sensitization, but we detected no differences in either DC expression of CD80, OX40L, or MHCII (Fig. S2 A), or T cell production of IFN-γ, IL-17A (Fig. 3, F and G), or other cytokines (Fig. 3 H and Fig. S2, B–D). The finding that adoptively transferring WT in vitro–generated αMHC-presenting BMDCs (Eriksson et al., 2003) to *Il3*−/− mice did not give rise to fulminant inflammation (Fig. 3, I and J) further substantiated the

idea that attenuated inflammation in *Il3*−/− mice occurred downstream of DC sensitization capacity. Thus, T cell sensitization in autoimmune myocarditis does not require IL-3.

Monocyte-derived APCs promote local T cell proliferation in the inflamed heart

Our data indicate that IL-3 is critical to leukocyte accumulation in the heart during myocarditis, but is dispensable to sensitization. Given IL-3's known role in leukocyte production (Weber et al., 2015), we enumerated leukocytes in the BM, blood, and spleen on days 0, 14, and 21 and found no differences between WT and *Il3*−/− mice (Fig. S2, E and F), suggesting that the leukocyte differences in the heart did not depend on altered hematopoiesis in the BM. We therefore turned our attention to the heart. The first evidence supporting a local function for IL-3 was the rate of local CD4+ T cell proliferation in the hearts of WT and *Il3*−/− mice: on day 21 after EAM induction, when WT hearts were producing abundant IL-3 (Fig. 2 A), we observed a marked reduction of local
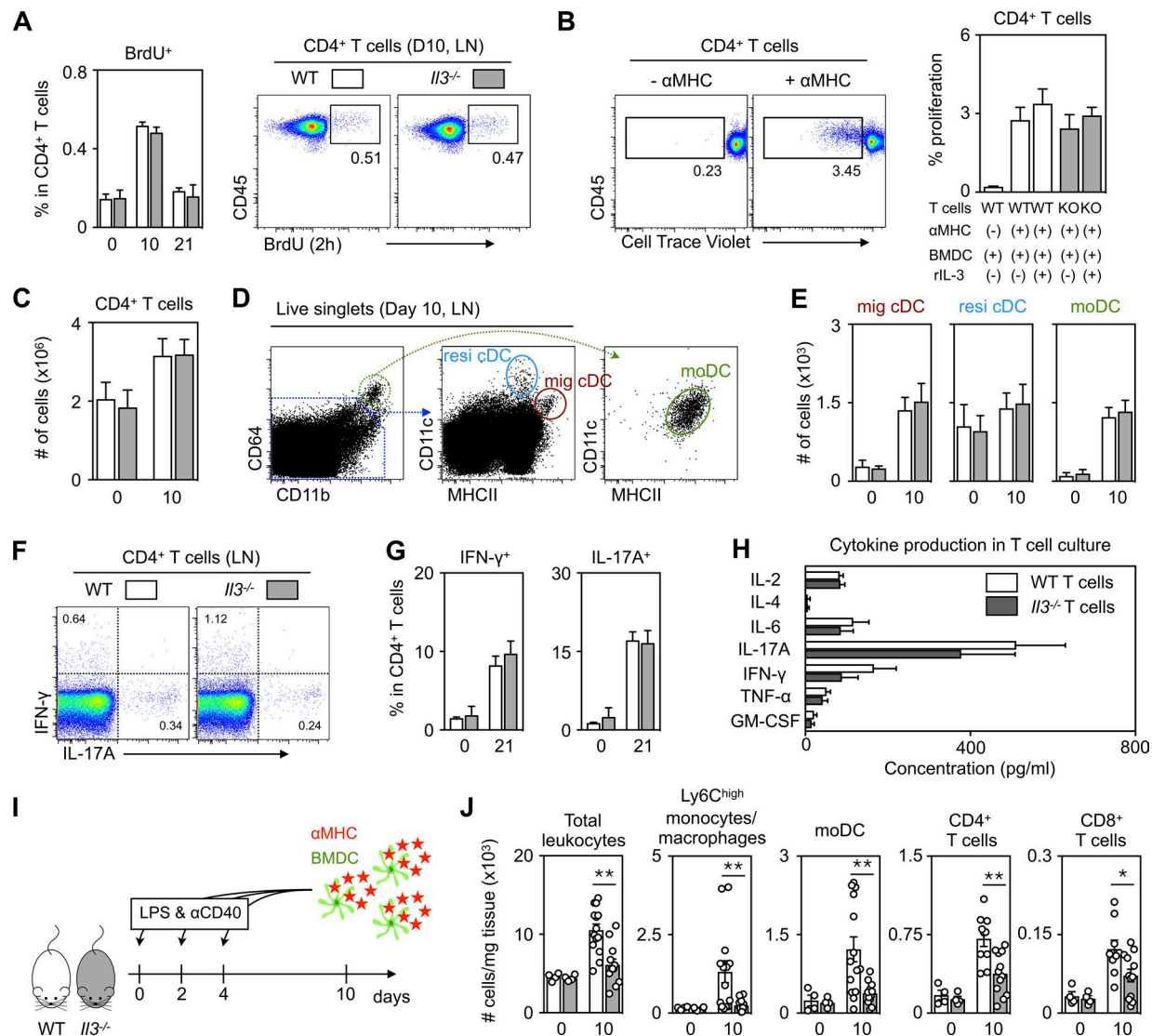
Anzai et al.
IL-3 in autoimmune myocarditis

Journal of Experimental Medicine

372

https://doi.org/10.1084/jem.20180722

Figure 3. **IL-3 is dispensable for T cell sensitization. (A)** In vivo T cell proliferation in the draining LNs was measured by BrdU incorporation before and 10 and 21 d after the first immunization (*n* = 4–8 per group of two independent experiments). BrdU was injected intraperitoneally 2 h before the sacrifice. **(B)** In vitro T cell proliferation was assessed by a cell tracer dye, Cell Trace Violet. CD4+ T cells obtained from LNs of immunized WT or *Il3*−/− mice were stained with Cell Trace Violet and cultured at indicated conditions for 72 h (*n* = 4–8 per group of three independent experiments). **(C)** Enumeration of CD4+ T cell numbers in the draining LNs before and 10 d after the first immunization (*n* = 4–8 per group of two independent experiments). **(D)** Representative flow dot plots to identify DC subsets in the draining LNs. **(E)** Quantification of migratory cDCs, resident cDCs, and moDCs in WT and *Il3*−/− draining LNs on days 0 and 10 (*n* = 4 per group of two independent experiments). **(F)** Production of IFN-γ and IL-17A by WT and *Il3*−/− CD4+ T cells in the draining LNs on day 21. **(G)** Percentage of IFN-γ+ or IL-17A+ CD4+ T cells in the draining LNs on day 21 (*n* = 4–8 per group of two independent experiments). **(H)** CD4+ T cells collected from draining LNs of immunized WT or *Il3*−/− mice were cultured with BMDC in the presence of 10 µg/ml αMHC for 3 d, and indicated cytokines were measured in the supernatants (*n* = 4–8 per group of two independent experiments). **(I)** Schematic diagram of the experimental design for BMDC-induced EAM. **(J)** Flow cytometry–based quantification of indicated cells in the hearts of WT and *Il3*−/− mice 10 d after the first BMDC injection (*n* = 4–14 per group grouped from at least two independent experiments). *, P < 0.05; **, P < 0.01. For statistical analysis, a two-tailed Mann–Whitney *U* test or unpaired *t* test was applied to compare two groups. Results are shown as mean ± SEM.

CD4+ T cell proliferation in *Il3*−/− mice (Fig. 4, A and B), which is in line with reduced CD4+ T cell numbers on day 21 after EAM (Fig. 1 G). This finding contrasted with day 10, an early time point with minimal IL-3 production, on which we found similar CD4+ T cell numbers (Fig. 1 G) and less proliferation, with no differences between the groups (Fig. 4 B). Notably, the 2-h pulse-chase window can assess local proliferation, because no BrdU+ cells yet appear in the blood (Fig. 4 B). Local proliferation rather than increased survival appeared to drive cell expansion, as we did not

detect any differences in T cell death, as assessed by caspase-3 (Fig. 4, C and D). Consequently, hearts of *Il3*−/− mice accumulated fewer CD4+ T cells, corresponding to overall fewer IFN-γ+, IL-17+, and GM-CSF+ cells (Fig. 4 E), and thus diminished inflammation.

To explore what accounted for local T cell proliferation, we first employed ex vivo approaches and found that CD4+ T cells proliferated robustly when cultured with antigen-loaded DCs sorted from myocarditis hearts, that absence of either DC or antigen reduced proliferation, and that recombinant IL-3 supple-
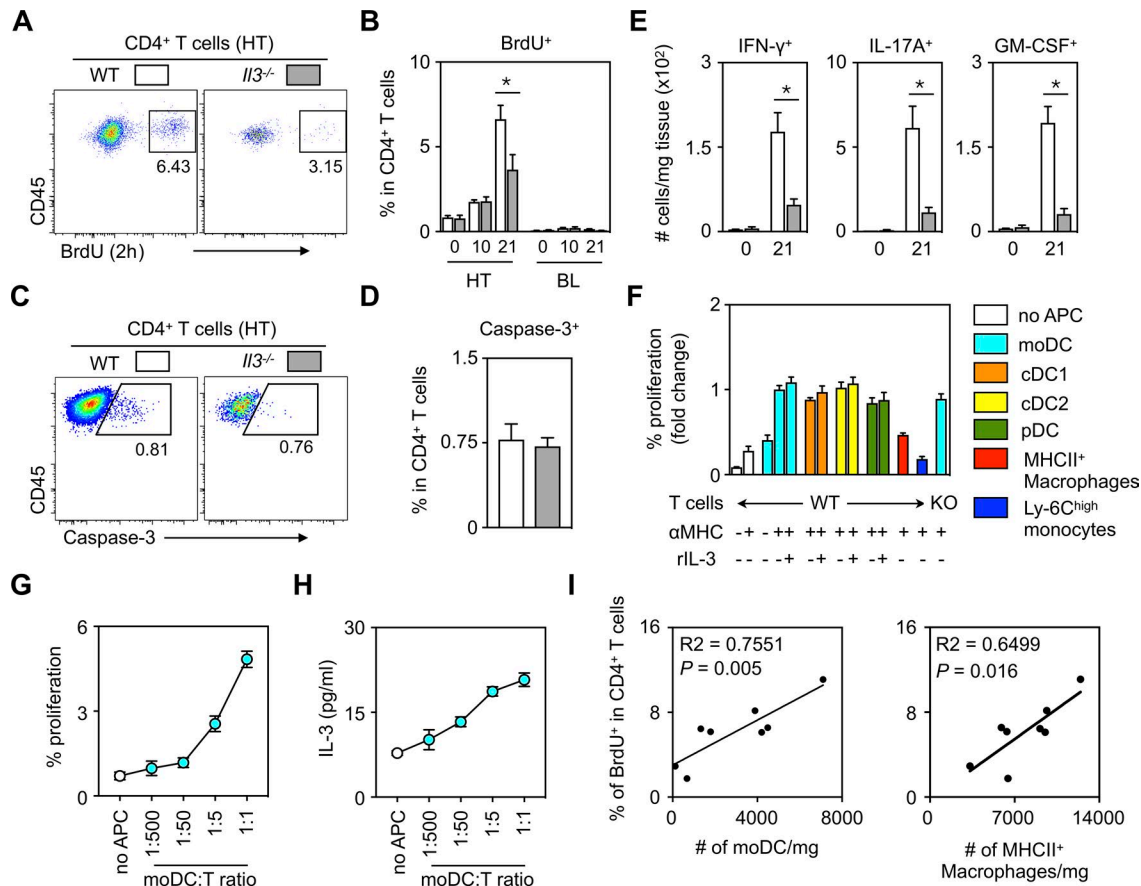
Figure 4. **Monocyte-derived APCs promote local T cell proliferation in the inflamed heart. (A)** CD4+ T cell proliferation was measured by BrdU incorporation in the inflamed hearts (HT) and blood of WT and *Il3*−/− mice 21 d after the first immunization. BrdU was injected 2 h before the sacrifice. **(B)** Percentage of BrdU+ cells in cardiac and blood (BL) CD4+ T cells of WT and *Il3*−/− mice at the indicated time points (*n* = 4–8 per group of two independent experiments). **(C)** Representative flow cytometric dot plots of activated caspase-3 expression in WT and *Il3*−/− CD4+ T cells in the heart 21 d after the first immunization. **(D)** Percentage of activated caspase-3+ cells shown in C (*n* = 4 per group of two independent experiments). **(E)** Quantification of IFN-γ+, IL-17A+, and GM-CSF+ CD4+ T cells in the hearts on days 0 and 21 (*n* = 4–8 per group of two independent experiments). **(F)** 5 × 10⁴ of autoreactive T cells and 10⁴ of each of the sorted cardiac populations were cultured at indicated conditions for 3 d. The percentage of proliferating T cells was evaluated by Cell Trace Violet dye and normalized to T cells cultured with moDCs in the presence of αMHC peptide (*n* = 4–7 per group of three independent experiments). **(G)** T cells sorted from day 14 draining LNs were stained with Cell Trace Violet and cultured with sorted cardiac moDCs at the indicated ratio. T cell proliferation was assessed 3 d later (*n* = 4 per group of two independent experiments). **(H)** IL-3 protein levels were measured by ELISA in the supernatant of the culture as in G (*n* = 4 per group of two independent experiments). **(I)** Correlation between T cell proliferation and the number of moDCs or MHCII+ macrophages in WT hearts at peak of inflammation. *, P < 0.05. For statistical analysis, a two-tailed Mann–Whitney *U* test or unpaired *t* test was applied to compare two groups, and linear regression analyses were performed to assess the correlation between T cell proliferation and the number of monocyte-derived APCs. Results are shown as mean ± SEM.

mentation had no effect (Fig. 4 F). Indeed, T cells, which express negligible levels of CD123, the IL-3–specific receptor subunit α (IL-3Rα; http://www.immgen.org), did not use IL-3, as IL-3–deficient CD4+ T cells cultured with antigen-loaded DCs proliferated just as well as WT CD4+ T cells (Fig. 4 F). We therefore wondered whether local T cell proliferation depended on the number of DCs. Among the DC subsets accumulating in the heart, moDCs were particularly informative, as they were the most abundant in the inflamed heart and their numbers differed between WT and *Il3*−/− mice (in contrast, cDC1 and cDC2 numbers between WT and *Il3*−/− inflamed hearts did not differ, and cardiac inflammation did not require pDC, as determined by pDC depletion; Fig. 1 F and Fig. S3, A and B). Importantly, we found that both the extent of T cell proliferation (Fig. 4 G) and IL-3 supernatant levels (Fig. 4 H) correlated with moDC numbers, as proliferation and IL-3 production both rose with increased moDC frequency. We

also found a strong positive in vivo correlation between CD4+ T cell proliferation in the heart and the number of cardiac moDC (Fig. 4 I), indicating that moDC are likely the primary drivers of local T cell proliferation. The noticeable decrease among MHCII+ macrophages, which were abundant in the inflamed hearts of WT mice and highly reduced in *Il3*−/− mice (Fig. 1 F), suggested that MHCII+ macrophages could also contribute to local T cell proliferation within the inflamed cardiac tissue. Although sorted cardiac MHCII+ macrophages loaded with αMHC appeared to be less effective in stimulating autoreactive CD4+ T cell proliferation compared with sorted moDCs (Fig. 4 F), we noted a strong positive correlation between CD4+ T cell proliferation and MHCII+ macrophages in vivo (Fig. 4 I). Together, these data reveal that (i) in myocarditis hearts, CD4+ T cells produce IL-3; (ii) moDC and MHCII+ macrophage accumulation in the inflamed myocardium depends on IL-3; and (iii) T cells proliferate in response to
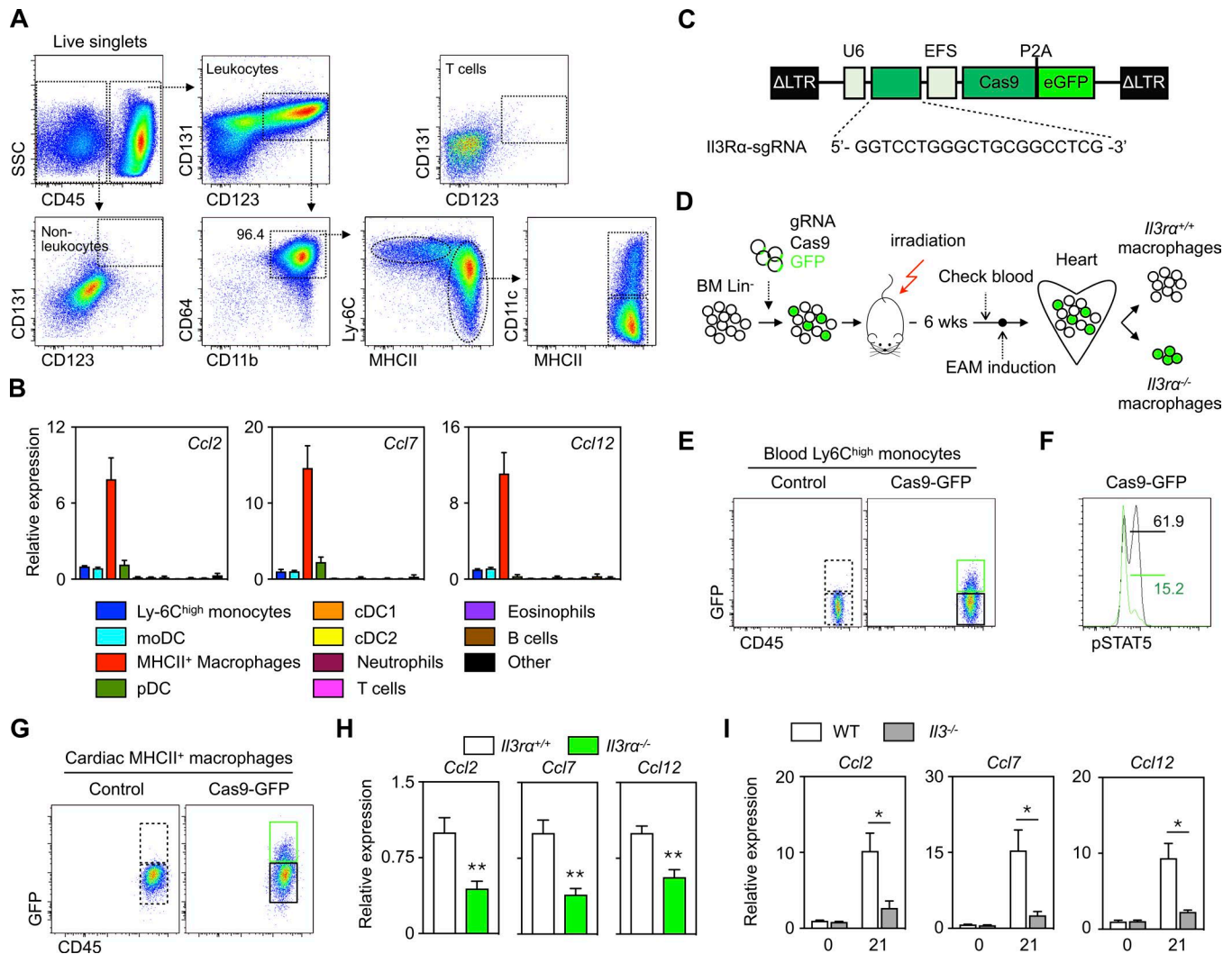
Figure 5. **IL-3 attracts monocytes by inducing cardiac macrophage chemokine production. (A)** Flow cytometric analysis for IL-3 receptor α subunit (IL-3Rα: CD123)–positive cells in the inflamed heart on day 21. Representative flow dot plots for CD123 as well as the β subunit of the receptor (CD131) are shown. **(B)** Comparison of *Ccl2*, *Ccl7*, and *Ccl12* gene expression in different leukocyte subsets sorted from WT myocarditis hearts on day 21. Values were normalized to that of Ly-6C^high monocytes (*n* = 4 per each population of two independent experiments). **(C)** Depiction of a lentiviral vector containing the sgRNA targeting IL-3Rα from a U6 promoter (U6) and Cas9 from a short EF1a promoter (EFS) with eGFP from a picornavirus-derived 2A autocleavage site (P2A). **(D)** Schematic diagram for experimental design. Lentiviral particles were transfected into BM lineage-negative (Lin⁻) cells, which were subsequently transferred into lethally irradiated WT mice, and myocarditis was induced 6 wk later. *Il3rα⁺/⁺* (GFP⁻) and *Il3rα⁻/⁻* (GFP⁺) cardiac macrophages were sorted at the peak of inflammation. **(E)** Representative flow dot plots to identify GFP⁺ cells in blood after gating on Ly-6C^high monocytes. **(F)** Phosphorylation of STAT5 after IL-3 stimulation, demonstrating lack of IL-3 receptor signaling in blood GFP⁺ cells. **(G)** Representative flow dot plots of cardiac macrophages in the inflamed heart to identify GFP⁺ cells. **(H)** Gene expression of *Ccl2*, *Ccl7*, and *Ccl12* in sorted IL-3Rα⁺/⁺ (GFP⁻) and IL-3Rα⁻/⁻ (GFP⁺) cardiac macrophages. **(I)** mRNA levels of indicated chemokines in the heart tissue of WT and *Il3⁻/⁻* mice before and 21 d after the first immunization (*n* = 4–9 per group of two independent experiments). *, P < 0.05; **, P < 0.01. For statistical analysis, a two-tailed Mann-Whitney *U* test or unpaired *t* test was applied to compare two groups. Results are shown as mean ± SEM.

accumulating antigen-loaded monocyte-derived APCs, but not directly in response to IL-3.

IL-3 attracts monocytes by inducing cardiac macrophage chemokine production

If moDC and macrophage accumulation in the heart depends on IL-3 (Fig. 1 F), then how does this occur? We first sought to identify the cells that can directly respond to IL-3. Analysis of leukocytes (Fig. 5 A) and non-leukocytes (endothelial cells, fibroblasts, and other stromal cells; Fig. S3 C) in the inflamed heart revealed the predominant IL-3R (CD123 and CD131)–expressing cells to be CD11b^high CD64^high MHCII⁺ CD11c⁻, a profile that is consistent with

cardiac macrophages, while non-leukocytes showed negligible numbers of cells expressing either subunit. Indeed, MHCII⁺ macrophages, DCs, and Ly-6C^high monocytes/macrophages, but not T cells or non-leukocytes, phosphorylated STAT5 in response to IL-3, indicating direct signaling downstream of the growth factor (Fig. S3 D). Although basophils prominently expressed IL-3R in the periphery, their accumulation into cardiac tissue was negligible at the peak of EAM (0.10 ± 0.01% in WT vs. 0.07 ± 0.03% in *Il3⁻/⁻* among CD45⁺ leukocytes; Fig. S3, E and F). Upon cell sorting, we noted that, among leukocytes, cardiac macrophages were by far the most abundant producers of the monocyte-attracting chemokines *Ccl2*, *Ccl7*, and *Ccl12* (Fig. 5 B).

Anzai et al.
IL-3 in autoimmune myocarditis

Journal of Experimental Medicine
https://doi.org/10.1084/jem.20180722

375

That said, we found that fibroblasts also produced monocyte chemoattractants in the inflamed myocardium, including *Ccl7* and *Ccl2* (Fig. S4 A), which agrees with previous studies showing that fibroblasts participate importantly in myocarditis (Lindner et al., 2014; Wu et al., 2014; Amoah et al., 2015). We therefore compared the relative abundance of cardiac macrophages and fibroblasts in naive and EAM mice and measured expression of *Ccl2*, *Ccl7*, and *Ccl12* in equal numbers of sorted cardiac MHCII+ macrophages and fibroblasts isolated from day 21 hearts (Fig. S4 B). We found that while cardiac fibroblasts were more numerous than cardiac macrophages in naive hearts, cardiac macrophages outnumbered fibroblasts in inflamed hearts. In addition, we found that cardiac MHCII+ macrophages expressed more *Ccl2* and *Ccl12* than fibroblasts on a per-cell level (Fig. S4 B). Thus, fibroblasts may be important IL-3–independent sources of monocyte chemoattractants, but macrophage-derived chemokines outnumber fibroblasts during myocarditis.

Next, we investigated IL-3–dependent myeloid expansion in more detail. Compared with WT mice, we observed no changes in myeloid cell proliferation, death, or chemokine receptor expression in *Il3−/−* mice, suggesting that IL-3–dependent myeloid expansion in the heart relied more on recruitment than on survival or local self-renewal (Fig. S4, C–E). This prompted us to ask whether IL-3 was stimulating IL-3R+ macrophages to produce monocyte-attracting chemokines. We elected to test for a direct IL-3–chemokine link with several approaches. First, we screened a macrophage cell line, J774, for IL-3R expression (Fig. S5 A) and cytokine production in response to IL-3 (Fig. S5 B), noting high induction of *Ccl2*, *Ccl7*, and *Ccl12*. Second, we sorted peritoneal macrophages, BM-derived macrophages, and cardiac MHCII+ macrophages from naive mice, stimulated the cells with IL-3, and again noted high increases of *Ccl2*, *Ccl7*, and *Ccl12* gene expression (Fig. S5 C). Importantly, we did not observe any changes in the expression of *Ccl2*, *Ccl7*, and *Ccl12* after stimulating sorted naive cardiac fibroblasts with IL-3 in vitro, which bolstered the idea that fibroblasts' production of monocyte chemoattractants is independent of IL-3 in EAM (Fig. S5 C). Third, we generated IL-3Rα–deficient cells using the CRISPR-Cas9 technique (Heckl et al., 2014) to answer the specific question of whether IL-3 stimulated cardiac macrophages in vivo. We designed a small guide RNA (sgRNA) targeting the IL-3–specific mouse IL-3Rα and integrated the RNA guide into a lentiviral vector that contained Cas9 and enhanced GFP (eGFP; Fig. 5 C). We validated the efficacy of the lentivirus/CRISPR approach using J774 cells in vitro, finding suppressed phosphorylation of STAT5 (Fig. S5, D and E) and reduced expression of *Ccl2*, *Ccl7*, and *Ccl12* in GFP+ cells, even after IL-3 stimulation (Fig. S5 F). We then transfected BM Lin− cells with the vector, transplanted the cells into lethally irradiated WT mice, and induced myocarditis after BM reconstitution (Fig. 5 D). Though the transfection was only ∼15% efficient, we did find a population of GFP+ Ly-6Chigh monocytes in the blood (Fig. 5 E) that, unlike their GFP− counterparts, failed to phosphorylate STAT5 upon IL-3 stimulation (Fig. 5 F), thereby confirming that GFP+ cells lacked a functional IL-3Rα. Finally, upon sorting, *Il3ra−/−* (GFP+) cardiac MHCIIhigh macrophages (Fig. 5 G) had reduced gene expression of the three key monocyte-attracting chemokines in the inflamed heart in comparison to *Il3ra+/+*

(GFP−) cardiac MHCIIhigh macrophages (Fig. 5 H). This observation corresponded with considerably less overall *Ccl2*, *Ccl7*, and *Ccl12* production in unsorted heart tissue of *Il3−/−* mice 21 d after EAM (Fig. 5 I). Thus, T cell–derived IL-3 locally acts on cardiac MHCIIhigh macrophages to produce monocyte-attracting chemokines during the course of myocarditis.

Interestingly, despite the reduced accumulation of neutrophils and T cells in the inflamed myocardium at the peak of EAM (Fig. 1, F and G), neutrophil (*Cxcl1* and *Cxcl2*) and T cell (*Ccl19* and *Ccl20*) chemoattractant expression was unchanged in our in vitro screening experiments involving IL-3 stimulation (Fig. S5 B). However, expression of *Cxcl1*, *Cxcl2*, and *Ccl19* was significantly decreased on day 21 in *Il3−/−* hearts (Fig. S5, G and H), suggesting that additional, yet-unidentified IL-3–dependent mechanisms indirectly promote neutrophil and T cell recruitment to the inflamed myocardium.

Anti-IL-3 therapy ameliorates acute inflammation and chronic fibrosis in myocarditis

Given IL-3's role in stimulating inflammation, we next wondered whether the cytokine can be targeted therapeutically to ameliorate myocarditis. Observations on specimens obtained from human hearts highlighted this question's potential clinical importance. We detected human *IL3* in two specimens collected from patients with myocarditis, but not from two commercially acquired samples of healthy human hearts ($4.718 \times 10^{-4} \pm 1.708 \times 10^{-4}$ vs. undetectable by qPCR). Intraperitoneally injecting anti-IL-3 antibody to presensitized animals attenuated leukocyte accumulation in the heart (Fig. 6 A), ameliorated inflammation, and decreased fibrosis at day 28 after the development of BMDC-induced EAM (Fig. 6 B). In addition, animals treated with anti-IL-3 antibody had improved cardiac function based on reduced left ventricular (LV) end-systolic diameter (LVESD) and elevated LV ejection fraction (LVEF; Fig. 6, C and D). Altogether, these data demonstrate the clinical relevance of IL-3. Since, as these data show, anti-IL-3 antibody can ameliorate inflammation, even in sensitized animals, it could be a useful therapeutic target for treating myocarditis. Ultimately, these results position IL-3 within the inflammatory cascade that occurs during autoimmune myocarditis as a critical factor that escalates the effector phase by inducing myeloid cell recruitment (Fig. 7).

Discussion

In this study, we identified and characterized an amplification loop, essential to autoimmune inflammation in myocarditis, that depends on the cytokine and growth factor IL-3. We show that IL-3–producing self-reactive effector CD4+ T cells incite tissue macrophages to produce monocyte-attracting chemokines, that newly recruited monocytes differentiate into monocyte-derived macrophages and DCs, and that the process repeats itself when DCs, upon encountering effector T cells in the tissue, stimulate local T cell proliferation.

The biological function of IL-3 has been predominantly studied in the context of mast cells, basophils, hematopoietic stem progenitor cells, and endothelial cells (Williams et al., 1990; Korpelainen et al., 1996; Lantz et al., 1998; Voehringer, 2013;
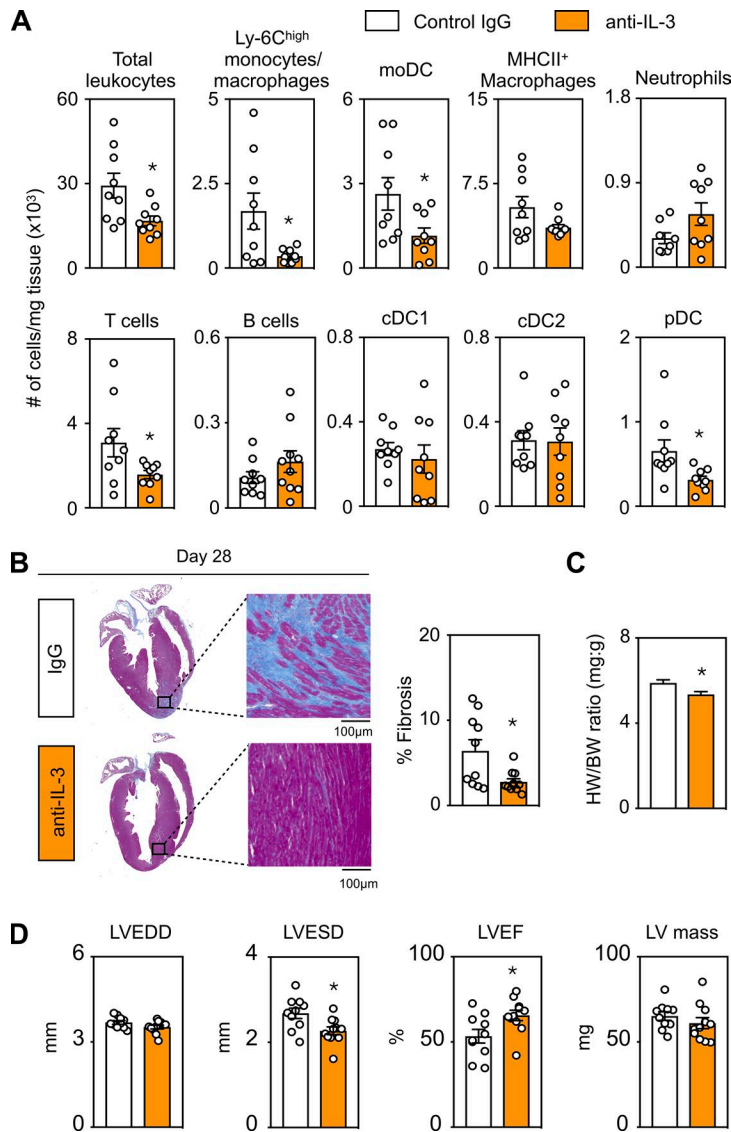
Anzai et al.
IL-3 in autoimmune myocarditis

Journal of Experimental Medicine   376
https://doi.org/10.1084/jem.20180722

A

Control IgG | anti-IL-3

Total leukocytes | Ly-6C^high monocytes/ macrophages | moDC | MHCII+ Macrophages | Neutrophils

T cells | B cells | cDC1 | cDC2 | pDC

# of cells/mg tissue (×10³)

B Day 28   **C**

IgG | anti-IL-3

100µm

% Fibrosis | HW/BW ratio (mg:g)

D

LVEDD | LVESD | LVEF | LV mass

mm | mm | % | mg

Weber et al., 2015). However, the cytokine's action on macrophages has been less explored. Likewise, although several studies have shown that IL-3 promotes certain kinds of autoimmune inflammation (Ito et al., 1997; Hofstetter et al., 2005; Brühl et al., 2009; Renner et al., 2015, 2016), its mechanism of action has remained elusive. For example, a previous study by Mack and colleagues using a mouse model of CIA reported IL-3's effects to be pathogenic during the early phase of CIA, whereby blockade with anti-IL-3 at disease onset reduced myeloid cell and basophil infiltration into synovial tissue, proinflammatory cytokine production, and histological joint scores (Brühl et al., 2009). On the other hand, Wani and colleagues reported that IL-3 suppressed CIA development through indirectly inducing regulatory T (T reg) cell expansion by stimulating IL-2 production via IL-3:IL-3R signaling on non–T reg cells (Srivastava et al., 2011). While different animal models, study conditions, and mechanisms controlling T reg cell differentiation and function could account for these contrasting results, our data ultimately align with models that have revealed a pathogenic role for IL-3 in promoting autoimmune inflammation and leukocyte accu-

mulation in the disease organ (Brühl et al., 2009; Renner et al., 2015, 2016).

The effector phase of autoimmune diseases such as autoimmune myocarditis is characterized by massive inflammation that involves recruitment of CCR2+ Ly-6C^high monocytes (Göser et al., 2005; Wu et al., 2014; Leuschner et al., 2015; Clemente-Casares et al., 2017). Our study places this phenomenon into a larger context of reciprocally controlled cellular function. On the one hand, the link between IL-3–producing T cells and monocyte recruitment reflects a functional hierarchy whereby effector T cells control monocyte recruitment in the effector tissue by stimulating resident macrophages. On the other hand, our data also show that accumulating monocytes, which are bipotential and can differentiate to fully functional moDCs and MHCII+ macrophages in cardiac tissue (Cheong et al., 2010; Epelman et al., 2014; Clemente-Casares et al., 2017; Van der Borght et al., 2017), influence T cells by stimulating their proliferation in a manner that is IL-3 dependent. This secondary reactivation in the effector organ is gaining interest and might play a role in disease relapse (Aloisi et al., 2000; Greter et al., 2005; Bailey
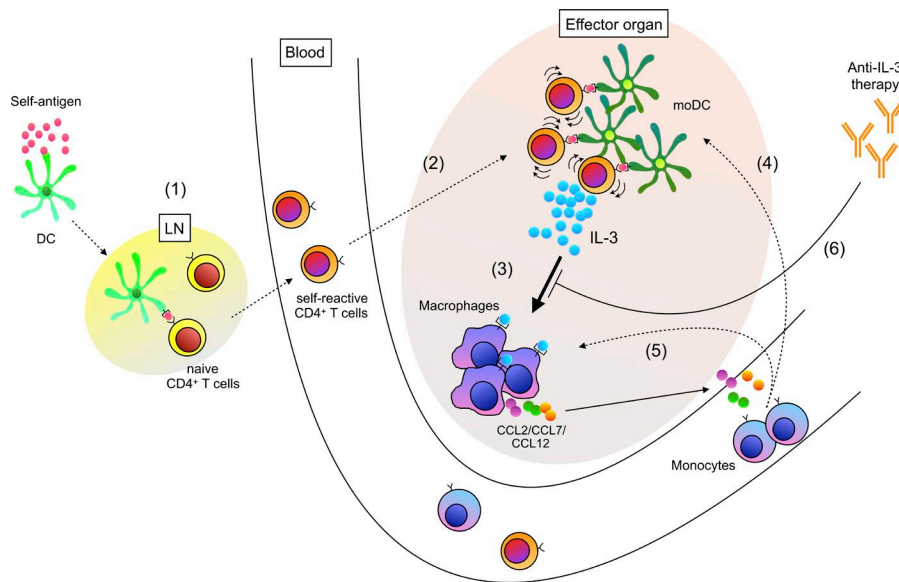
Figure 7. Proposed model. We propose that IL-3's function in autoimmune disease is as follows: During sensitization, DCs present self-antigen to T cells, and this process is IL-3 independent (1). Self-reactive T cells circulate and travel to their destination tissue, where they are reactivated by tissue APCs (2). T cell–derived IL-3 acts on macrophages to produce CCL2, CCL7, and CCL12 (3). Recruited CCR2+ Ly-6C^high monocytes differentiate into moDCs and MHCII+ macrophages that preferentially proliferate and activate T cells, leading to enhanced T cell proliferation and production of T cell–derived cytokines, including IL-3 (4). Monocytes also give rise to macrophages that further produce monocyte-attracting chemokines in response to IL-3 (5). This IL-3–dependent T cell–macrophage–moDC tricellular amplification loop is dismantled by anti-IL-3 treatment that mitigates tissue inflammation and damage (6).

et al., 2007; Becher et al., 2017). Indeed, in EAE, it has been shown that both CD11c+ DCs and Ly-6C+ monocyte precursors, which can differentiate into moDCs and macrophages, traffic to the central nervous system in a CCR2-dependent manner and are critical for disease progression (Izikson et al., 2000; King et al., 2009; Sagar et al., 2012a; Clarkson et al., 2015). While a role for central nervous system–infiltrating CCR2+ DCs in driving the accumulation of coinfiltrating, self-reactive T cells has been postulated in EAE (Wlodarczyk et al., 2014; Clarkson et al., 2015), how this process occurs upstream of CCR2-mediated recruitment in autoimmunity has remained unknown. Given our observations in EAM that IL-3 is responsible for directing the accumulation of moDCs and MHCII+ macrophages, which subsequently stimulate self-reactive CD4+ T cell proliferation and cytokine production during the peak of inflammation, it is plausible that IL-3 may also act analogously in other models of T cell–mediated autoimmune inflammation upstream of CCR2+ myeloid cell recruitment. Thus, uncontrolled inflammation occurs during the effector phase of autoimmune inflammation, our study suggests, not because one cell controls another but because of a positive IL-3–dependent reinforcement amplification loop that leads to a progressively larger leukocyte presence in the target organ.

It remains unclear whether IL-3–producing CD4+ T cells are a distinct Th cell lineage. On the one hand, it is possible the IL-3+ IFN-γ− IL-17A− CD4+ T cells identified in this study are a population of recently activated effector T cells that have yet to differentiate into other inflammatory Th lineages. On the other hand, they may instead be related to the recently described neuroinflammatory GM-CSF+ CD4+ T cells (Hartmann et al., 2014; Noster et al., 2014; Sheng et al., 2014). Future work is needed to identify any potential lineage-defining transcription factors that might support IL-3+ CD4+ T cell generation and lineage stability.

Our study's finding that IL-3 is produced in human myocarditis hearts, coupled with the observation in mice that IL-3 is an essential amplifier of inflammation in the effector organ, identifies

the cytokine as a potential therapeutic target to counteract T cell–driven cardiac tissue inflammation and fibrosis. Future work will show whether neutralizing IL-3 can be effective for treating viral myocarditis and other inflammatory cardiac complications, such as acute myocarditis and heart failure associated with checkpoint blockade immunotherapy (Swirski and Nahrendorf, 2018). IL-3, our study shows, contributes to this T cell–mediated inflammatory cascade, and though it may act downstream of sensitization, its profound effects on disease progression reveal it to be a major hub of influence.

Materials and methods

Mice

BALB/c (Taconic), C.129S7(B6)-Rag1tm1Mom/J, CByJ.B6-Tg(UBC-GFP)30Scha/J, CBySmn.CB17-Prkdcscid/J were purchased from The Jackson Laboratory. IL-3–deficient (Il3−/−) mice on a BALB/c background (nine generations) were bred in-house (Weber et al., 2015). All experiments were conducted with female mice unless otherwise indicated. All protocols were approved by the Animal Review Committee at Massachusetts General Hospital (Protocols 2011N000035 and 2015N000044) and by the Institutional Animal Care and Use Committee at the Keio University School of Medicine.

Animal models and in vivo interventions
EAM induction

Mice were subcutaneously injected with 100 µg cardiac αMHC (Ac-RSLKLMATLFSTYASADR-OH) peptide emulsified in CFA containing 1 mg/ml heat-killed *Mycobacterium tuberculosis H37Ra* (Sigma-Aldrich) on days 0 and 7 (Leuschner et al., 2015). Myocarditis was also achieved by αMHC-pulsed, activated BMDCs as previously described (Eriksson et al., 2003). In brief, BM cells were cultured in complete medium (RPMI-1640 medium supplemented with 10% FBS, 2 mM L-glutamine, 100 U/ml penicillin and streptomycin, 10 mM Hepes, 50 µM 2-mercaptoethanol, 1 mM sodium pyruvate, and 1× nonessential amino acids) supplemented with 10

ng/ml GM-CSF (PeproTech) for 6 d. After collecting nonadherent cells, CD11c$^+$ cells were enriched by magnetic separation. The cells were then pulsed with 10 µg/ml αMHC overnight and activated by 1 µg/ml LPS (Sigma–Aldrich) and 5 µg/ml of antibody against CD40 (BD Biosciences) for 4 h. Subsequently, 3–6 × 10^5 activated BMDCs were intraperitoneally injected into recipient mice on days 0, 2, and 4. In some experiments, spleen cells were collected from immunized WT or $Il3^{-/-}$ mice on day 14 and pulsed with 20 µg/ml αMHC for 72 h. CD4$^+$ T cells were isolated by magnetic separation, and 10^7 of these T cells were adoptively transferred into CBySmn.CB17-Prkdcscid/J (Scid) mice to induce myocarditis.

Adoptive transfer of GFP$^+$ monocytes
BM Ly-6C^{high} monocytes were obtained from CByJ.B6-Tg(UBC-GFP)30Scha/J mice by flow-assisted cell sorting after enrichment of cells negative for CD3, CD19, B220, CD49b, and Ly6G using magnetic cell separation. 15 d after the first immunization, 2 × 10^6 GFP$^+$ Ly-6C^{high} monocytes were injected intravenously into WT BALB/c mice, and GFP$^+$ cells in the inflamed heart were assessed 2 d later.

BM transplantation
Naive WT BALB/c mice were lethally irradiated (500 cGy twice, 4 h apart) and reconstituted with a mixture of BM cells obtained from $Rag1^{-/-}$ and either WT or $Il3^{-/-}$ mice to generate $Rag1^{-/-}$/WT and $Rag1^{-/-}$/$Il3^{-/-}$ BM mixed chimeras. After 6–7 wk to allow for reconstitution, the mice were subjected to EAM induction, and leukocyte populations in the heart were evaluated by flow cytometry on day 21.

BrdU incorporation experiments
To assess cell proliferation, 1 mg BrdU was injected intraperitoneally 2 h before euthanasia and subsequent organ harvest. A BrdU flow kit (BD Biosciences) was used to stain BrdU$^+$ cells.

pDC depletion
WT BALB/c mice were randomly assigned to either the control IgG or anti-CD317 antibody (300 µg; clone BX444; Bio X Cell)–injecting group and subjected to BMDC-induced myocarditis. The antibodies were intraperitoneally injected into mice every other day from 1 d before the first BMDC injection.

Anti–IL-3 neutralization antibody treatment
After injection of activated BMDCs pulsed with αMHC into WT mice on days 0, 2, and 4, mice were randomly allocated to either the anti-IL-3–treated group or the control IgG-treated group. Neutralizing antibody against IL-3 (100 µg; clone MP2-8F8; Bio X Cell) or control IgG1 (100 µg; clone HRPN; Bio X Cell) was intraperitoneally injected once a day for 7 d.

Echocardiography
Transthoracic echocardiography was performed with a Vevo 2100 instrument (VisualSonics) equipped with an MS-400 imaging transducer. M-mode tracings were recorded through the anterior and posterior LV walls at the papillary muscle level to measure LV end-diastolic diameter (LVEDD), LVESD, and LVEF. LV mass was assessed to evaluate cardiac hypertrophy.

Cell isolation
Peripheral blood was collected by retro-orbital bleeding, and erythrocytes were lysed in RBC lysis buffer (BioLegend). Spleen, draining LNs, femurs, tibia, and heart were excised after vascular perfusion with cold PBS. Minced spleen and LNs and flushed BM were strained through 40-µm nylon mesh (BD Biosciences) and further subjected to RBC lysis. The naive and inflamed hearts were minced and digested with 450 U/ml collagenase I, 125 U/ml collagenase XI, 60 U/ml DNase I, and 60 U/ml hyaluronidase (Sigma-Aldrich) in PBS for 1 h at 37°C while shaking. For cell sorting, single-cell suspensions of heart tissue from indicated animals were made as described above and stained to identify indicated cell populations. Cells were sorted on a FACS Aria II cell sorter (BD Biosciences) directly into either RLT lysis buffer (Qiagen) for subsequent RNA isolation or complete medium for cell culture experiments.

Flow cytometry
Single-cell suspensions were stained in PBS supplemented with sterile 2% FBS and 0.5% BSA. The following monoclonal antibodies were used for flow cytometric analysis: anti-CD45 (30-F11), anti-CD3 (clone 145-2C11), anti-CD4 (clone RM4-5), anti-CD8 (clone 53–6.7), anti-CD90.2 (clone 53–2.1), anti-B220 (clone RA3-6B2), anti-Ly6G (clone 1A8), anti-Ly-6C (AL-21), anti-I-A/I-E (MHCII; clone M5/114.15.2), anti-CD11b (clone M1/70), anti-CD11c (clone HL3), anti-CD64 (clone X54-5/7.1), anti-CD103 (clone 2E7), anti-PDCA1 (clone 927), anti-CD62L (clone MEL-14), anti-CD80 (clone 16-10A1), anti-OX40L (clone RM134L), anti-CD123 (clone REA114), anti-CD131 (clone REA193), anti-CD31 (clone 390), anti-Feeder (MEFSK4; clone mEF-SK4), anti-CD192 (CCR2; clone 475301; clone SA203G11), anti-F4/80 (clone BM8), anti-CD115 (CSF-1R; clone AFS98), anti-Siglec-F (clone E50-2440), anti-CD24 (clone M1/69), anti-CD26 (clone H194-112), anti-XCR1 (clone ZET), anti-CD172a (SIRPα; clone P84), anti-Zbtb46 (clone U4-1374), anti-CD117 (c-Kit; clone 2B8), anti-IgE (clone RME-1), anti-FcεRIα (clone MAR-1), anti-CD49b (clone DX5), anti-IL-3 (clone MP2-8F8), anti-IL-4 (clone 11B11), anti-IFNγ (clone XMG1.2), anti-IL-17A (clone TC11-18H10.1), anti-GM-CSF (clone MP1-22E9), anti-activated caspase-3 (clone C92-605), anti-pSTAT5 (clone pY694), and isotype controls. Antibodies were purchased from BioLegend, BD Biosciences, eBioscience, or Miltenyi Biotec. Viable cells were identified as unstained cells with Zombie Aqua (BioLegend).

Staining strategies
For intracellular cytokine staining, cell suspensions were stimulated in 2% FBS RPMI-1640 medium with 100 ng/ml PMA and 1 µg/ml ionomycin (Sigma-Aldrich) in the presence of GolgiStop and GolgiPlug (BD Biosciences) for 3–4 h at 37°C, 5% CO$_2$ before fixation and permeabilization. Staining for pSTAT5 was performed as previously described (Anzai et al., 2017). In brief, cells were stimulated with or without recombinant murine IL-3 (20 ng/ml; PeproTech) for 30 min at 37°C to induce phosphorylation of STAT5, followed by addition of 4% PFA solution (pH 7.4) to obtain a final concentration of 2%. After fixation for 20 min, cells were resuspended in 1 ml ice-cold methanol to permeabilize. After 30 min of incubation at 4°C, cells were washed twice

Anzai et al.
IL-3 in autoimmune myocarditis

Journal of Experimental Medicine
https://doi.org/10.1084/jem.20180722

379

and stained with anti-pSTAT5 antibody as well as antibodies for extracellular antigens for 45 min at room temperature before a final wash and acquisition. For proliferation assays, CD4^{+} T cells were labeled with Cell Tracer Violet (Thermo Fisher Scientific), and proliferating cells were identified as Cell Tracer Violet-dim. Data were acquired on a BD LSRII and analyzed with FlowJo (Tree Star).

Cell culture
WT and $Il3^{-/-}$ mice were subjected to CFA-induced EAM induction, and autoreactive T cells were isolated from draining LNs on day 14. Cardiac APCs such as moDCs, cDC1, cDC2, and pDCs, as well as MHCII[high] macrophages and Ly-6C^{high} monocytes/macrophages, were sorted from the heart at peak inflammation, and BMDCs were generated as described above. 5×10^5 T cells with 10^5 BMDCs or 5×10^4 T cells with 10^4 sorted cardiac APCs were cultured in 200 µl complete medium with or without 10 µg/ml αMHC for 72 h in a humidified 5% CO_2 incubator at 37°C. The supernatants were collected, and indicated cytokines were measured by ELISA as described below. For the T cell proliferation assay, T cells were stained with Cell Trace Violet before incubation according to the manufacturer's instruction. Recombinant murine IL-3 (20 ng/ml; PeproTech) was added to some culture wells. To evaluate the effect of IL-3 on macrophages, J774 macrophage cell lines (Sigma-Aldrich), peritoneal macrophages, BMDMs, and sorted cardiac MHCII^{+} macrophages (CD64^{+} MHCII^{+} Ly-6C^{−} F4/80^{+}) from naive mice were used. Peritoneal macrophages were obtained as previously described (Rauch et al., 2012). To prepare BMDMs, BM cells were isolated from adult WT BALB/c mice and cultured in complete medium supplemented with 10 ng/ml recombinant murine M-CSF (PeproTech) for 8 d. The macrophage cell lines and primary cells were stimulated with or without 20 ng/ml recombinant IL-3 for 8 h and subjected to mRNA isolation as described below.

Generation of IL-3Rα–deficient cells by CRISPR-Cas9
LentiCRISPRv2GFP was a gift from David Feidser (University of Pennsylvania, Philadelphia, PA; plasmid 82416; http://n2t .net/addgene:82416; RRID:Addgene_82416; Addgene). sgRNA targeting mouse IL-3Rrα (5′-GGTCCTGGGCTGCGGCCTCG-3′) was cloned into the vector using Golden Gate assembly with BsmBI restriction enzyme. Validation of sgRNA was performed by flow cytometric analysis for phosphorylation of STAT5 after IL-3 stimulation. To generate lentivirus particles, plasmids (LentiCRISPRv2GFP-IL-3Rα, pMD2G, psPAX2) were cotransfected to HEK 293T cells, and supernatant was collected 48 h after the transfection. Following filtration (40 µm), virus particles were concentrated with ultracentrifugation at the speed of 20,000 rpm for 3 h. Subsequently, virus pellet was suspended with medium without aeration. To generate IL-3Rα–deficient cells in vivo, BM lineage–negative cells were isolated from adult BALB/c mice using EasySep Mouse hematopoietic progenitor cell isolation kit (STEMCELL Technologies) according to the manufacturer's instruction. The isolated progenitor cells were cultured in StemSpan (STEMCELL Technologies) supplemented with 50 ng/ml murine Tpo and 50 ng/ml murine Scf (both PeproTech) for 1 h and then transduced with concentrated lentiviral supernatant.

16 h after transduction, cells were collected and transplanted into lethally irradiated (500 cGy, twice, 4 h apart) WT BALB/c mice. After 6 wk of recovery, either EAM was induced.

Histopathology
Immunized mice were euthanized, and hearts were removed, embedded in Tissue-Tek O.C.T. compound (Sakura Finetek), frozen in 2-methylbutane (Fisher Scientific) cooled with dry ice, and sectioned into 6-µm slices. H&E staining was used to assess acute cardiac inflammation, which was evaluated by histopathological microscopic approximation of the percent area of myocardium infiltrated with mononuclear cells. To assess cardiac fibrosis, fibrotic area was quantified in 5–10 randomly selected fields of view per Azan-stained sample by ImageJ software.

Reverse transcriptional PCR
Tissue
Mouse total RNA was isolated using the RNeasy Mini Kit (Qiagen) according to the manufacturer's instructions. cDNA was generated from 1 µg of total RNA per sample using High Capacity cDNA Reverse Transcription Kit (Applied Biosystems). Human myocardial tissue samples were obtained from two patients with confirmed myocarditis and one patient with normal myocardium, frozen, and kept in the Brigham Research Institute tissue bank at Brigham and Women's Hospital. Those tissues were approved by Institutional Review Board Protocol 1999P991348/BWH. Total RNA and cDNA extraction were performed as described above. Two additional control heart total RNA were also obtained from Thermo Fisher Scientific (lot number 1906770 and 1866106), followed by generation of cDNA.

Cells
5×10^3 Ly-6C^{high} monocytes/macrophages, moDC, MHCII[high] macrophages, pDC, cDC1, cDC2, neutrophils, T cells, eosinophils, B cells, and other leukocytes and 2×10^4 total leukocytes, endothelial cells, fibroblasts, and other stromal cells were sorted from inflamed heart, and total RNA was extracted using the RNeasy Micro Kit (Qiagen) followed by cDNA transcription. Quantitative real-time TaqMan PCR was performed using following TaqMan primers (Applied Biosystems): Il3 (Mm00439631_m1), Il1α (Mm00439620_m1), Il1β (Mm01336189_m1), Il6 (Mm00446190_m1), Il10 (Mm01288386_m1), Il22 (Mm01226722_g1), Il23a (Mm00518984_m1), Tnf (Mm00443258_m1), Tgfβ (Mm01227699_m1), Mmp2 (Mm00439498_m1), Mmp9 (Mm00442991_m1), Csf2 (Mm01290062_m1), Vegf (Mm00437306_m1), Cxcl1 (Mm04207460_m1), Cxcl2 (Mm00436450_m1), Ccl2 (Mm00441242_m1), Ccl3 (Mm00441259_g1), Ccl5 (Mm01302427_m1), Ccl7 (Mm00443113_m1), Ccl12 (Mm01617100_m1), Ccl19 (Mm00839967_g1), Ccl20 (Mm01268754_m1), Ccl24 (Mm00444701_m1), Bax (Mm00432051_m1), Bim (Mm00437796_m1), Bcl2 (Mm00477631_m1), Il3rα (Mm00434273_m1), and housekeeping gene Gapdh (Mm99999915_g1). PCR was run on a 7500 Fast Real-Time PCR system (Applied Biosystems). Gene expression was calculated relative to *Gapdh* and normalized to controls. Human *IL3* gene expression data were quantified by $2^{-\Delta CT}$, and mouse gene expression data were calculated by the $2^{-\Delta\Delta CT}$ method.

Anzai et al.
IL-3 in autoimmune myocarditis

Journal of Experimental Medicine
https://doi.org/10.1084/jem.20180722

380

ELISA

IL-3 levels were measured in cell culture supernatants with the Mouse IL-3 ELISA Kit (R&D Systems or Boster Biological). IL-2, IL-4, IL-6, IL-17A, IFN-γ, TNF-α, and GM-CSF levels were also measured in cell culture supernatants with ELISA Kits from R&D Systems according to the manufacturer's instructions. High-sensitivity mouse troponin I ELISA kit (Life Diagnostics) was used to measure serum cardiac troponin I after EAM induction.

Statistics

GraphPad Prism 8.0 (GraphPad Software) was used for statistical analyses for all experiments. Results are shown as mean ± SEM. Data were analyzed for normality using the D'Agostino–Pearson test. Statistical tests included unpaired, two-tailed nonparametric Mann–Whitney U tests (when Gaussian distribution was not assumed) and two-tailed unpaired t tests for normally distributed data. For multiple comparisons, nonparametric multiple comparisons test comparing mean rank of each group (when Gaussian distribution was not assumed) or one-way ANOVA followed by Tukey's test was performed. P values of ≤0.05 were considered significant.

Online supplemental material

Fig. S1 shows that $Il3^{-/-}$ male mice are likewise protected from EAM inflammation and depicts flow cytometric profiling for identifying inflammatory cell subsets in the inflamed heart. Fig. S2 shows that IL-3 does not affect T cell sensitization and peripheral leukocyte numbers in EAM. Fig. S3 shows that pDC depletion does not affect cardiac leukocyte numbers during EAM and depicts the cell sorting strategy for non-leukocytes, pSTAT5 activity in leukocyte subsets by flow cytometry, and assessment of IL-3 receptor expression and basophil quantification in the periphery and inflamed heart by flow cytometry. Fig. S4 shows the profiling chemokine expression in different cell subsets in myocarditis and IL-3's effects on proliferation, apoptosis, and chemokine receptor expression in myeloid cells. Fig. S5 shows how IL-3 enhances monocyte-attracting chemokine expression in macrophages.

References

Aloisi, F., F. Ria, and L. Adorini. 2000. Regulation of T-cell responses by CNS antigen-presenting cells: different roles for microglia and astrocytes. *Immunol. Today.* 21:141–147. https://doi.org/10.1016/S0167-5699(99)01512-1

Ammirati, E., M. Cipriani, M. Lilliu, P. Sormani, M. Varrenti, C. Raineri, D. Petrella, A. Garascia, P. Pedrotti, A. Roghi, et al. 2017. Survival and Left Ventricular Function Changes in Fulminant Versus Nonfulminant Acute Myocarditis. *Circulation.* 136:529–545. https://doi.org/10.1161/CIRCULATIONAHA.117.026386

Amoah, B.P., H. Yang, P. Zhang, Z. Su, and H. Xu. 2015. Immunopathogenesis of Myocarditis: The Interplay Between Cardiac Fibroblast Cells, Dendritic Cells, Macrophages and CD4+ T Cells. *Scand. J. Immunol.* 82:1–9. https://doi.org/10.1111/sji.12298

Anzai, A., J.L. Choi, S. He, A.M. Fenn, M. Nairz, S. Rattik, C.S. McAlpine, J.E. Mindur, C.T. Chan, Y. Iwamoto, et al. 2017. The infarcted myocardium solicits GM-CSF for the detrimental oversupply of inflammatory leukocytes. *J. Exp. Med.* 214:3293–3310. https://doi.org/10.1084/jem.20170689

Bailey, S.L., B. Schreiner, E.J. McMahon, and S.D. Miller. 2007. CNS myeloid DCs presenting endogenous myelin peptides 'preferentially' polarize CD4+ T(H)-17 cells in relapsing EAE. *Nat. Immunol.* 8:172–180. https://doi.org/10.1038/ni1430

Becher, B., S. Spath, and J. Goverman. 2017. Cytokine networks in neuroinflammation. *Nat. Rev. Immunol.* 17:49–59. https://doi.org/10.1038/nri.2016.123

Bluestone, J.A., H. Bour-Jordan, M. Cheng, and M. Anderson. 2015. T cells in the control of organ-specific autoimmunity. *J. Clin. Invest.* 125:2250–2260. https://doi.org/10.1172/JCI78089

Brühl, H., J. Cihak, M. Niedermeier, A. Denzel, M. Rodriguez Gomez, Y. Talke, N. Goebel, J. Plachý, M. Stangassinger, and M. Mack. 2009. Important role of interleukin-3 in the early phase of collagen-induced arthritis. *Arthritis Rheum.* 60:1352–1361. https://doi.org/10.1002/art.24441

Cheong, C., I. Matos, J.H. Choi, D.B. Dandamudi, E. Shrestha, M.P. Longhi, K.L. Jeffrey, R.M. Anthony, C. Kluger, G. Nchinda, et al. 2010. Microbial stimulation fully differentiates monocytes to DC-SIGN/CD209(+) dendritic cells for immune T cell areas. *Cell.* 143:416–429. https://doi.org/10.1016/j.cell.2010.09.039

Cihakova, D., and N.R. Rose. 2008. Pathogenesis of myocarditis and dilated cardiomyopathy. *Adv. Immunol.* 99:95–114. https://doi.org/10.1016/S0065-2776(08)00604-4

Clarkson, B.D., A. Walker, M.G. Harris, A. Rayasam, M. Sandor, and Z. Fabry. 2015. CCR2-dependent dendritic cell accumulation in the central nervous system during early effector experimental autoimmune encepha-

Anzai et al.
IL-3 in autoimmune myocarditis

Journal of Experimental Medicine 381
https://doi.org/10.1084/jem.20180722

lomyelitis is essential for effector T cell restimulation in situ and disease progression. *J. Immunol.* 194:531–541. https://doi.org/10.4049/jimmunol.1401320

Clemente-Casares, X., S. Hosseinzadeh, I. Barbu, S.A. Dick, J.A. Macklin, Y. Wang, A. Momen, C. Kantores, L. Aronoff, M. Farno, et al. 2017. A CD103+ Conventional Dendritic Cell Surveillance System Prevents Development of Overt Heart Failure during Subclinical Viral Myocarditis. *Immunity.* 47:974–989.e8. https://doi.org/10.1016/j.immuni.2017.10.011

Cooper, L.T. Jr. 2009. Myocarditis. *N. Engl. J. Med.* 360:1526–1538. https://doi.org/10.1056/NEJMra0800028

Dardalhon, V., T. Korn, V.K. Kuchroo, and A.C. Anderson. 2008. Role of Th1 and Th17 cells in organ-specific autoimmunity. *J. Autoimmun.* 31:252–256. https://doi.org/10.1016/j.jaut.2008.04.017

Epelman, S., K.J. Lavine, A.E. Beaudin, D.K. Sojka, J.A. Carrero, B. Calderon, T. Brija, E.L. Gautier, S. Ivanov, A.T. Satpathy, et al. 2014. Embryonic and adult-derived resident cardiac macrophages are maintained through distinct mechanisms at steady state and during inflammation. *Immunity.* 40:91–104. https://doi.org/10.1016/j.immuni.2013.11.019

Eriksson, U., R. Ricci, L. Hunziker, M.O. Kurrer, G.Y. Oudit, T.H. Watts, I. Sonderegger, K. Bachmaier, M. Kopf, and J.M. Penninger. 2003. Dendritic cell-induced autoimmune heart failure requires cooperation between adaptive and innate immunity. *Nat. Med.* 9:1484–1490. https://doi.org/10.1038/nm960

Fairweather, D., L.T.J. Cooper Jr., and L.A. Blauwet. 2013. Sex and gender differences in myocarditis and dilated cardiomyopathy. *Curr. Probl. Cardiol.* 38:7–46. https://doi.org/10.1016/j.cpcardiol.2012.07.003

Goodnow, C.C., J. Sprent, B. Fazekas de St Groth, and C.G. Vinuesa. 2005. Cellular and genetic mechanisms of self tolerance and autoimmunity. *Nature.* 435:590–597. https://doi.org/10.1038/nature03724

Göser, S., R. Ottl, A. Brodner, T.J. Dengler, J. Torzewski, K. Egashira, N.R. Rose, H.A. Katus, and Z. Kaya. 2005. Critical role for monocyte chemoattractant protein-1 and macrophage inflammatory protein-1alpha in induction of experimental autoimmune myocarditis and effective anti-monocyte chemoattractant protein-1 gene therapy. *Circulation.* 112:3400–3407. https://doi.org/10.1161/CIRCULATIONAHA.105.572396

Greter, M., F.L. Heppner, M.P. Lemos, B.M. Odermatt, N. Goebels, T. Laufer, R.J. Noelle, and B. Becher. 2005. Dendritic cells permit immune invasion of the CNS in an animal model of multiple sclerosis. *Nat. Med.* 11:328–334. https://doi.org/10.1038/nm1197

Hapel, A.J., J.C. Lee, W.L. Farrar, and J.N. Ihle. 1981. Establishment of continuous cultures of thy1.2+, Lyt1+, 2- T cells with purified interleukin 3. *Cell.* 25:179–186. https://doi.org/10.1016/0092-8674(81)90242-7

Hartmann, F.J., M. Khademi, J. Aram, S. Ammann, I. Kockum, C. Constantinescu, B. Gran, F. Piehl, T. Olsson, L. Codarri, and B. Becher. 2014. Multiple sclerosis-associated IL2RA polymorphism controls GM-CSF production in human TH cells. *Nat. Commun.* 5:5056. https://doi.org/10.1038/ncomms6056

Heckl, D., M.S. Kowalczyk, D. Yudovich, R. Belizaire, R.V. Puram, M.E. McConkey, A. Thielke, J.C. Aster, A. Regev, and B.L. Ebert. 2014. Generation of mouse models of myeloid malignancy with combinatorial genetic lesions using CRISPR-Cas9 genome editing. *Nat. Biotechnol.* 32:941–946. https://doi.org/10.1038/nbt.2951

Hofstetter, H.H., A.Y. Karulin, T.G. Forsthuber, P.A. Ott, M. Tary-Lehmann, and P.V. Lehmann. 2005. The cytokine signature of MOG-specific CD4 cells in the EAE of C57BL/6 mice. *J. Neuroimmunol.* 170:105–114. https://doi.org/10.1016/j.jneuroim.2005.09.004

Ihle, J.N., L. Pepersack, and L. Rebar. 1981. Regulation of T cell differentiation: in vitro induction of 20 alpha-hydroxysteroid dehydrogenase in splenic lymphocytes from athymic mice by a unique lymphokine. *J. Immunol.* 126:2184–2189.

Ito, A., N. Aoyanagi, and T. Maki. 1997. Regulation of autoimmune diabetes by interleukin 3-dependent bone marrow-derived cells in NOD mice. *J. Autoimmun.* 10:331–338. https://doi.org/10.1006/jaut.1997.0142

Izikson, L., R.S. Klein, I.F. Charo, H.L. Weiner, and A.D. Luster. 2000. Resistance to experimental autoimmune encephalomyelitis in mice lacking the CC chemokine receptor (CCR)2. *J. Exp. Med.* 192:1075–1080. https://doi.org/10.1084/jem.192.7.1075

King, I.L., T.L. Dickendesher, and B.M. Segal. 2009. Circulating Ly-6C+ myeloid precursors migrate to the CNS and play a pathogenic role during autoimmune demyelinating disease. *Blood.* 113:3190–3197. https://doi.org/10.1182/blood-2008-07-168575

Korpelainen, E.I., J.R. Gamble, M.A. Vadas, and A.F. Lopez. 1996. IL-3 receptor expression, regulation and function in cells of the vasculature. *Immunol. Cell Biol.* 74:1–7. https://doi.org/10.1038/icb.1996.1

Kronenberg, M., and A. Rudensky. 2005. Regulation of immunity by self-reactive T cells. *Nature.* 435:598–604. https://doi.org/10.1038/nature03725

Lantz, C.S., J. Boesiger, C.H. Song, N. Mach, T. Kobayashi, R.C. Mulligan, Y. Nawa, G. Dranoff, and S.J. Galli. 1998. Role for interleukin-3 in mast-cell and basophil development and in immunity to parasites. *Nature.* 392:90–93. https://doi.org/10.1038/32190

Leuschner, F., G. Courties, P. Dutta, L.J. Mortensen, R. Gorbatov, B. Sena, T.I. Novobrantseva, A. Borodovsky, K. Fitzgerald, V. Koteliansky, et al. 2015. Silencing of CCR2 in myocarditis. *Eur. Heart J.* 36:1478–1488. https://doi.org/10.1093/eurheartj/ehu225

Lindner, D., J. Li, K. Savvatis, K. Klingel, S. Blankenberg, C. Tschöpe, and D. Westermann. 2014. Cardiac fibroblasts aggravate viral myocarditis: cell specific coxsackievirus B3 replication. *Mediators Inflamm.* 2014:519528. https://doi.org/10.1155/2014/519528

Marrack, P., J. Kappler, and B.L. Kotzin. 2001. Autoimmune disease: why and where it occurs. *Nat. Med.* 7:899–905. https://doi.org/10.1038/90935

Mohan, J.F., and E.R. Unanue. 2012. Unconventional recognition of peptides by T cells and the implications for autoimmunity. *Nat. Rev. Immunol.* 12:721–728. https://doi.org/10.1038/nri3294

Noster, R., R. Riedel, M.F. Mashreghi, H. Radbruch, L. Harms, C. Haftmann, H.D. Chang, A. Radbruch, and C.E. Zielinski. 2014. IL-17 and GM-CSF expression are antagonistically regulated by human T helper cells. *Sci. Transl. Med.* 6:241ra80. https://doi.org/10.1126/scitranslmed.3008706

Rauch, P.J., A. Chudnovskiy, C.S. Robbins, G.F. Weber, M. Etzrodt, I. Hilgendorf, E. Tiglao, J.L. Figueiredo, Y. Iwamoto, I. Theurl, et al. 2012. Innate response activator B cells protect against microbial sepsis. *Science.* 335:597–601. https://doi.org/10.1126/science.1215173

Renner, K., F.J. Hermann, K. Schmidbauer, Y. Talke, M. Rodriguez Gomez, G. Schiechl, J. Schlossmann, H. Brühl, H.J. Anders, and M. Mack. 2015. IL-3 contributes to development of lupus nephritis in MRL/lpr mice. *Kidney Int.* 88:1088–1098. https://doi.org/10.1038/ki.2015.196

Renner, K., S. Hellerbrand, F. Hermann, C. Riedhammer, Y. Talke, G. Schiechl, M.R. Gomez, S. Kutzi, D. Halbritter, N. Goebel, et al. 2016. IL-3 promotes the development of experimental autoimmune encephalitis. *JCI Insight.* 1:e87157. https://doi.org/10.1172/jci.insight.87157

Rosenblum, M.D., K.A. Remedios, and A.K. Abbas. 2015. Mechanisms of human autoimmunity. *J. Clin. Invest.* 125:2228–2233. https://doi.org/10.1172/JCI78088

Sagar, D., A. Lamontagne, C.A. Foss, Z.K. Khan, M.G. Pomper, and P. Jain. 2012a. Dendritic cell CNS recruitment correlates with disease severity in EAE via CCL2 chemotaxis at the blood-brain barrier through paracellular transmigration and ERK activation. *J. Neuroinflammation.* 9:245. https://doi.org/10.1186/1742-2094-9-245

Sagar, S., P.P. Liu, and L.T. Cooper Jr. 2012b. Myocarditis. *Lancet.* 379:738–747. https://doi.org/10.1016/S0140-6736(11)60648-X

Sheng, W., F. Yang, Y. Zhou, H. Yang, P.Y. Low, D.M. Kemeny, P. Tan, A. Moh, M.H. Kaplan, Y. Zhang, and X.Y. Fu. 2014. STAT5 programs a distinct subset of GM-CSF-producing T helper cells that is essential for autoimmune neuroinflammation. *Cell Res.* 24:1387–1402. https://doi.org/10.1038/cr.2014.154

Srivastava, R.K., G.B. Tomar, A.P. Barhanpurkar, N. Gupta, S.T. Pote, G.C. Mishra, and M.R. Wani. 2011. IL-3 attenuates collagen-induced arthritis by modulating the development of Foxp3+ regulatory T cells. *J. Immunol.* 186:2262–2272. https://doi.org/10.4049/jimmunol.1002691

Swirski, F.K., and M. Nahrendorf. 2018. Cardioimmunology: the immune system in cardiac homeostasis and disease. *Nat. Rev. Immunol.* 18:733–744. https://doi.org/10.1038/s41577-018-0065-8

Theofilopoulos, A.N., D.H. Kono, and R. Baccala. 2017. The multiple pathways to autoimmunity. *Nat. Immunol.* 18:716–724. https://doi.org/10.1038/ni.3731

Trachtenberg, B.H., and J.M. Hare. 2017. Inflammatory Cardiomyopathic Syndromes. *Circ. Res.* 121:803–818. https://doi.org/10.1161/CIRCRESAHA.117.310221

Van der Borght, K., C.L. Scott, V. Nindl, A. Bouché, L. Martens, D. Sichien, J. Van Moorleghem, M. Vanheerswynghels, S. De Prijck, Y. Saeys, et al. 2017. Myocardial Infarction Primes Autoreactive T Cells through Activation of Dendritic Cells. *Cell Reports.* 18:3005–3017. https://doi.org/10.1016/j.celrep.2017.02.079

Voehringer, D. 2013. Protective and pathological roles of mast cells and basophils. *Nat. Rev. Immunol.* 13:362–375. https://doi.org/10.1038/nri3427

Weber, G.F., B.G. Chousterman, S. He, A.M. Fenn, M. Nairz, A. Anzai, T. Brenner, F. Uhle, Y. Iwamoto, C.S. Robbins, et al. 2015. Interleukin-3 ampli-

fies acute inflammation and is a potential therapeutic target in sepsis. *Science.* 347:1260–1265. https://doi.org/10.1126/science.aaa4268

Williams, G.T., C.A. Smith, E. Spooncer, T.M. Dexter, and D.R. Taylor. 1990. Haemopoietic colony stimulating factors promote cell survival by suppressing apoptosis. *Nature.* 343:76–79. https://doi.org/10.1038/343076a0

Wlodarczyk, A., M. Løbner, O. Cédile, and T. Owens. 2014. Comparison of microglia and infiltrating CD11c⁺ cells as antigen presenting cells for T cell proliferation and cytokine response. *J. Neuroinflammation.* 11:57. https://doi.org/10.1186/1742-2094-11-57

Wu, L., S. Ong, M.V. Talor, J.G. Barin, G.C. Baldeviano, D.A. Kass, D. Bedja, H. Zhang, A. Sheikh, J.B. Margolick, et al. 2014. Cardiac fibroblasts mediate IL-17A-driven inflammatory dilated cardiomyopathy. *J. Exp. Med.* 211:1449–1464. https://doi.org/10.1084/jem.20132126

Yang, Y.C., A.B. Ciarletta, P.A. Temple, M.P. Chung, S. Kovacic, J.S. Witek-Giannotti, A.C. Leary, R. Kriz, R.E. Donahue, G.G. Wong, et al. 1986. Human IL-3 (multi-CSF): identification by expression cloning of a novel hematopoietic growth factor related to murine IL-3. *Cell.* 47:3–10. https://doi.org/10.1016/0092-8674(86)90360-0